



Scholars Research Library

Der Pharmacia Lettre, 2016, 8 (9):258-268
(<http://scholarsresearchlibrary.com/archive.html>)



Application of bimetallic Zn-Ag nanoparticles embedded in MMT-biopolymer nanobiocomposites for the removal of monocrotophos from aqueous environment: Equilibrium, kinetic and thermodynamic studies

Sahithya K. and Nilanjana Das*

School of Biosciences and Technology, VIT University, Vellore-632014, India

ABSTRACT

The present study investigates the efficiency of bimetallic zinc-silver (Zn-Ag) nanoparticles embedded in montmorillonite (MMT)-biopolymer viz., Zn-Ag/MMT/Chitosan (Ch), Zn-Ag/MMT/Gum ghatti (Gg) and Zn-Ag/MMT/Poly lactic acid (PLA) nanobiocomposites for the removal of monocrotophos (MCP) from aqueous solution. The composites were characterized by XRD, TGA, and BET. The parameters viz., pH, contact time, temperature, initial concentration and dosage were optimized. The removal of MCP followed the order: Zn-Ag/MMT/PLA (98.8%) > Zn-Ag/MMT/Ch (90.7%) > Zn-Ag/MMT/Gg (86.9%) > Zn-Ag/MMT (64.8%). The adsorption of MCP onto composites was well explained by Freundlich model. The kinetic studies suggested that the adsorption of MCP on composites proceeds according to pseudo-first order. Intraparticle diffusion and Boyd plot suggested that the film diffusion was not the sole rate limiting step. Thermodynamic parameters of adsorption were also determined. The mechanism of adsorption process was also elucidated by FT-IR, AFM and EDX. Furthermore, regeneration studies showed that the adsorbent could be reused up to six cycles.

Key words: Adsorption, Biopolymers, Monocrotophos (MCP), Montmorillonite (MMT), Zinc-silver nanoparticles.

INTRODUCTION

Monocrotophos [dimethyl (E)-1-methyl-2-(methylcarbamoyl)vinyl phosphate, MCP] is one of the most popular and broadly used organophosphate insecticide owing to its high efficiency and low cost in controlling pests mainly on cotton crop, sugarcane, rice and other vegetable crops in India [1]. WHO and EPA classified MCP in class I- highly toxic compound, which is identified as endocrine disrupting chemical [2]. As an exogenous agent present in the environment, MCP disrupts the endocrine functions, such as growth, development and reproduction in humans, animals and birds. MCP is extremely toxic to honey bees and moderately toxic to fishes even at a low concentration [3]. Exposure to MCP is known to produce a variety of biochemical dysfunctions in mammals causing high irritation to the eyes, slurred speech, loss of reflexes, weakness, involuntary muscle contractions, and paralysis of the body [4]. Though it is banned on the usage in edible crops in India from 2006, it is illegally used on all crops [5]. It is one of the highest consumed pesticides in India and has a half life of approximately 66 days at neutral pH [6,7]. The levels of MCP above maximum residue limits ($0.2 \mu\text{g g}^{-1}$) in various vegetables have been reported [8]. Several reports have highlighted the existence of MCP and its residues in surface, ground and rain water via point and non-point sources [9,10].

Several techniques such as microbial degradation [11], Fenton degradation [12] and photocatalytic degradation [13] are being practiced to remove the pesticides from aqueous solution. However, these techniques are associated with major limitations such as time consuming, high cost and generation of residual products [14]. Thus, there is a need to search for a cost effective and eco-friendly technique for the efficient removal of MCP from aqueous environment. Adsorption is proven to be suitable, effective and economical method for the elimination of wide

range of contaminants from aqueous solution [15]. Several research reports highlighted the application of various adsorbents for the removal of pesticides from aqueous environment [16-19].

In recent years, biopolymer-clay based nanobiocomposites have become a subject of intensive research due to their ability of nanoscale dispersion in biopolymer matrix, which brings significant improvement in physical and functional properties of both the biopolymers and nanoparticles [20]. Biopolymers have been reported as a promising class of materials for removal of various organic or inorganic compounds from wastewater due to their improved properties such as non-toxicity and biodegradability [21]. Clays have been widely used as nanofillers in biopolymer systems due to low cost and improved mechanical properties of the nanobiocomposites. In addition, clays are well known for their high binding capacities due to the higher surface area and unique layered structure [22,23]. Recent reports suggested the application of various biopolymer-clay nanobiocomposites for the removal of pesticides [24-26]. However, no report is available on use of nanobiocomposite composed of bimetallic nanoparticles, biopolymer and clay minerals.

In the present study the efficiency of nanobiocomposite composed of bimetallic Zn-Ag nanoparticles, montmorillonite, chitosan, gum ghatti and poly lactic acid were evaluated with respect to achievable MCP adsorption from aqueous environment. The composites were characterized using XRD, BET and TGA. The adsorption mechanism was elucidated using FT-IR, AFM and EDX. In addition, desorption and regeneration experiments were conducted in batch studies.

MATERIALS AND METHODS

All the chemicals were analytical grade and used without further purification. Monocrotophos (MCP, purity 99.9%), chitosan of high molecular weight (Ch), gum ghatti (Gg), poly lactic acid (PLA) and montmorillonite (MMT, clay) with surface area of 20-40 m² g⁻¹ were purchased from Sigma Aldrich Chemicals, India. The standard solution of MCP (1000 mg L⁻¹) was prepared using deionised water and the experimental solutions were obtained by successive dilutions of standard MCP solution.

Synthesis of Zn-Ag/MMT nanocomposite

Zinc-silver bimetallic nanoparticles/MMT nanocomposite were synthesised using a simple oxido-reduction method described by Srivatsan *et al.*, [27] with minor modifications. Briefly, 10 % (w/v) montmorillonite was dispersed in 80 ml solution containing 240 mg of porcine gelatine. Zn(NO₃)₂ solution (10 mmol/5 ml 0.01 N) solution was added to the above suspension followed by AgNO₃ (10 mmol/5 ml H₂O). After the reaction of 10 min, the pH was raised to 9.5 using 1 N NaOH and the solution was stirred for 2 h at 60 °C. The precipitate formed was centrifuged, washed three times with deionised water and freeze dried at 60 °C to obtain a fine powder of nanocomposite.

Preparation of Zn-Ag/MMT-biopolymer nanobiocomposites

Chitosan based nanobiocomposite (Zn-Ag/MMT/Ch) was prepared by adding 10 % (w/v) Zn-Ag/MMT nanocomposite in 100 ml containing 2 % (v/v) glacial acetic acid and magnetically stirred for 30 min at room temperature. Chitosan (2 %) was added to the above suspension and the mixture was stirred for 60 min to obtain a homogenous suspension after which the suspension was dried at 60 °C for 4 h.

Gum ghatti based nanobiocomposite (Zn-Ag/MMT/Gg) was prepared by addition of 1 % (w/v) gum in 100 ml distilled water containing 10 % (w/v) Zn-Ag/MMT nanocomposite. The pH of the solution was maintained at 4.0 using 1N HCl. The suspension was left overnight allowing the swelling of gum in the solution and dried at 60 °C for 4 h.

Poly lactic acid based nanobiocomposite (Zn-Ag/MMT/PLA) was prepared following the same procedure described for the preparation of Zn-Ag/MMT/Ch. In the present case, acetic acid and chitosan were replaced by chloroform and poly lactic acid respectively.

Characterization

X-ray diffraction (XRD) patterns of the bimetallic Zn-Ag nanoparticles were recorded on Bruker D8 Advance diffractometer with Cu-K α radiation in the 2 θ range of 20°-80° with a scanning rate of 4 min and step size of 0.02. The thermal behaviour of composites was studied using the thermogravimetric analyser under helium atmosphere at a heating rate of 10 °C min⁻¹ and differential scanning calorimetry. The BET surface areas of composites were calculated following the standard procedure [28]. The point zero charge (pH_{PZC}) of composites was evaluated following the standard method [29].

Spectroscopic studies

The involvement of various functional groups in adsorption of MCP was studied using FT-IR spectra recorded on Avatar 330 model FT-IR spectrophotometer (Thermo Nicolet Co., USA). The surface elemental composition of composites was analysed using Noran System Six model Energy Dispersive X-ray Microanalysis System (Thermo Electron Corporation, Japan). Accelerating voltage was kept constant at 15 kV, to facilitate the emission of secondary X-rays. The surface topologies of composites before and after adsorption were analysed using Atomic force microscope (Nanosurf easyscan-2, Netherlands).

Adsorption experiments

The batch adsorption experiments were carried out in duplicates and the results were reported as an average. For adsorption experiments, a known weight of adsorbent was mixed with 50 ml of MCP solutions in Erlenmeyer flask at room temperature ($26 \pm 2^\circ\text{C}$) and shaken for a set period of time. The effect of operating parameters *viz.*, pH (4.0-11.0), contact time (30-390 min), reaction temperature ($10-50^\circ\text{C}$), initial MCP concentration ($20-160 \text{ mg L}^{-1}$) and adsorbent dosage ($1.0-6.0 \text{ mg L}^{-1}$) were investigated. At the end of pre-determined time interval, the samples were centrifuged at 10,000 rpm for 10 min and the supernatant was analysed for the residual MCP concentrations using high performance liquid chromatography (HPLC). The uptake capacity (q) of adsorbent and the removal percentage (R) of MCP were calculated using the following equations.

$$q = \frac{C_0 - C_f}{M} \times V$$
$$R = \frac{C_0 - C_f}{C_0} \times 100$$

Where, C_0 (mg L^{-1}) and C_f (mg L^{-1}) are the MCP concentrations before and after adsorption respectively; V (L) is the volume of MCP solutions and M (g) is the weight of the adsorbents.

Equilibrium, Kinetics and thermodynamic studies

The equilibrium data were analysed by using two-parameter isotherms Langmuir, Freundlich and Dubinin-Radushkevich (D-R) models. The kinetic experiments were conducted at optimum conditions and samples were withdrawn at equal intervals for analysis. Pseudo-first order, Pseudo-second order, Intraparticle diffusion and Boyd plot have been used for the modelling of the kinetic data for adsorption of MCP on nanobiocomposites. The fundamental thermodynamic parameters such as Gibbs free energy (ΔG), enthalpy (ΔH) and entropy (ΔS) were calculated to evaluate the thermodynamic feasibility and the nature of the adsorption process using standard equations.

Desorption and regeneration experiments

Desorption experiments were carried out with composite initially treated with $50 \mu\text{g mL}^{-1}$ solution of pesticide during the adsorption study. After reaching the adsorption equilibrium, solutions were filtered and the composite was resuspended in deionised water. The resuspended samples were shaken at $30 \pm 2^\circ\text{C}$, after which the suspensions were centrifuged and the desorbed pesticide was analysed as reported in the section 6.0. Desorption procedure was repeated three times for each composite. All experiments were carried out in triplicates and results were reported as an average. Composites after desorption of pesticide was regenerated by drying at 60°C for 4 h. The adsorption, desorption and regeneration cycle was repeated eight times using the same composite.

RESULTS AND DISCUSSION

Characterization

X-ray diffraction patterns of nanoparticles were determined in the range of $20-80^\circ$ and the results are presented in Fig. 1. The XRD pattern of both the ZnO and Ag nanoparticles exhibited a well defined peak thereby, indicating their purity. The XRD pattern of ZnO nanoparticles had peaks at 2θ values of 31.7, 34.4, 36.2, 47.5, 56.5, 62.8 and 67.9 which correspond to the 100, 002, 101, 102, 110, 103 and 112 planes respectively (Fig. 1a). For the Ag nanoparticles, the peaks obtained were at 2θ values of 38.0, 44.2, 64.3 and 77.3 which correspond to the 111, 200, 220 and 311 planes respectively (Fig. 1b). The intensity of the ZnO peaks at 2θ values of 31.7, 36.25 and 56.5 reflected high degree of crystallinity in nanoparticles. In case of Ag, peaks at 2θ values of 38.0 and 64.3 indicated high degree of crystallinity in Ag nanoparticles. The diffraction peaks obtained for bimetallic Zn-Ag nanoparticles had corresponding characteristic peaks which were obtained in both the individual nanoparticles which suggested the co-existence of both Zn and Ag nanoparticles (Fig. 1c). It was also noted that, bimetallic Zn-Ag nanoparticles

retain their respective crystalline structures as seen in the individual nanoparticles, suggesting the interaction of one metal on the other forming a bimetallic nano-complex of ZnO and Ag.

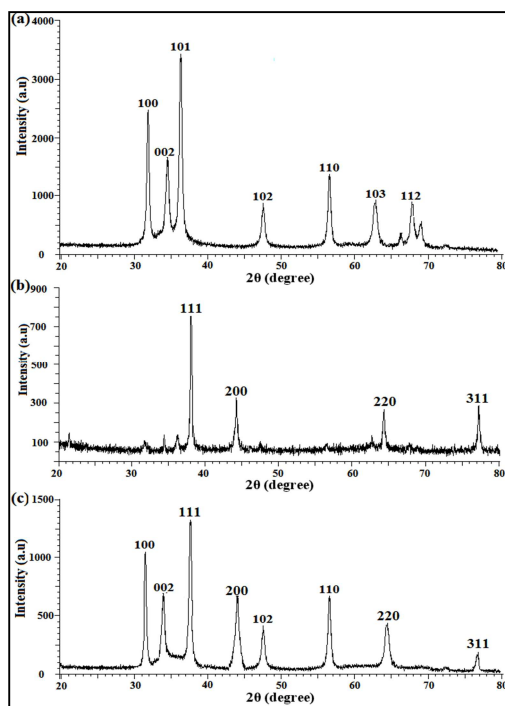


Figure 1: X-ray diffraction pattern of (a) ZnO nanoparticles, (b) Ag nanoparticles and (c) bimetallic Zn-Ag nanoparticles

The surface areas of the composites viz. Zn-Ag/MMT/PLA, Zn-Ag/MMT/Ch, Zn-Ag/MMT/Gg and Zn-Ag/MMT were measured as $78 \text{ m}^2 \text{ g}^{-1}$, $66 \text{ m}^2 \text{ g}^{-1}$, $43 \text{ m}^2 \text{ g}^{-1}$ and $38 \text{ m}^2 \text{ g}^{-1}$ respectively by BET. TGA analysis suggested a lower weight loss percentage in case of Zn-Ag/MMT/PLA (22.7 %) followed by Zn-Ag/MMT/Ch (29.3 %), Zn-Ag/MMT/Gg (41.5 %) and Zn-Ag/MMT (49.9 %).

The pH_{PZC} is major characteristic of any adsorbent as it indicates the net surface charge of the adsorbent in solution. The pH_{PZC} values of Zn-Ag/MMT, Zn-Ag/MMT/Ch, Zn-Ag/MMT/Gg and Zn-Ag/MMT/PLA was found to be 5.6, 6.9, 5.7 and 6.2 respectively which suggested the composites possess positive charge below the pH_{PZC} and negative charge above the pH_{PZC} .

Effect of parameters

The pH of the solution plays an important role on pesticides adsorption since it controls the magnitude of electrostatic charges and degree of ionization of the pesticides. The effect of pH on the removal of MCP was examined in pH range 4.0 to 11.0 and the data is presented in Fig. 2(a). The acidic conditions favoured the adsorption of MCP molecules by all the composites. Maximum removal was noted at pH 5.0 and 6.0 by Zn-Ag/MMT, Zn-Ag/MMT/Gg and Zn-Ag/MMT/PLA, Zn-Ag/MMT/Ch respectively. The pH dependency on removal efficiencies could be explained based on the surface charge of the composites (pH_{PZC}) and degree of ionisation of MCP (pK_a). The pK_a of MCP is 4.4 which signify that the MCP exist as positively charged cation and above the same, negatively charged MCP anions predominates [30]. The high adsorption efficiency at optimum pH values clearly suggests the electrostatic attraction between positively charged composites surface and negatively charged MCP anions in the solution. The decrease in MCP removal in alkaline pH range was due to the electrostatic repulsion between the negatively charged composites surface and MCP anions.

Removal of MCP by composites as a function of contact time is depicted in Fig. 2(b). The effect of contact time on MCP adsorption was studied ranging from 30 to 390 min. The removal efficiency of Zn-Ag/MMT/Ch, Zn-Ag/MMT/PLA and Zn-Ag/MMT, Zn-Ag/MMT/Gg composites reached equilibrium at 120 and 180 min respectively. It was observed that the adsorption of MCP was significantly rapid in the initial stages due to abundant availability of active sites on composites surface and with gradual occupancy of these sites, the adsorption becomes less efficient in the later stages [31].

The influence of temperature on the removal of MCP from the aqueous solution was investigated at temperatures ranging from 10 to 50 °C. As shown in Fig. 2(c) an increase in temperature from 10 to 30 °C increased the

adsorption of MCP by all the composites. The decrease in MCP adsorption efficiency by all the composites at high temperature was due to the high solubility of the pesticide that could be less retained by the binding site of composite thereby affecting the overall adsorption process [32,33].

The influence of initial MCP concentration on the adsorption of MCP was carried out by varying the MCP concentration ranging from 20 to 160 mg L⁻¹. Maximum uptake was noted at 80 mg L⁻¹ by Zn-Ag/MMT nanocomposite and Zn-Ag/MMT/Gg nanobiocomposite whereas Zn-Ag/MMT/Ch and Zn-Ag/MMT/PLA showed at 100 mg L⁻¹ and 120 mg L⁻¹ respectively (Fig. 2d). The adsorption of MCP was found to increase with increase in initial pesticide concentration due to the availability of more number of MCP molecules for adsorption process [34]. However, a further increase in initial MCP concentration showed significant decrease in removal due to the repulsive forces between the MCP molecules those are bound to adsorbent and those are present in the solution.

The effect of composite dosage on MCP removal efficiency is presented in Fig. 2(e) and the effect of composite concentration was studied in the range of 1.0 to 6.0 g L⁻¹. Maximum MCP removal was noted at 5.0 g L⁻¹ and 3.0 g L⁻¹ in case of Zn-Ag/MMT nanocomposite and other nanobiocomposites respectively. The enhanced removal along with the increase in composite dosage was due to the availability of exchangeable ions and increased number of active sites on the composites surface [35]. The removal efficiency was found to be decreased beyond the optimum concentration which could be due to aggregation of composite materials thereby leading to a decreased surface area for the MCP adsorption [36].

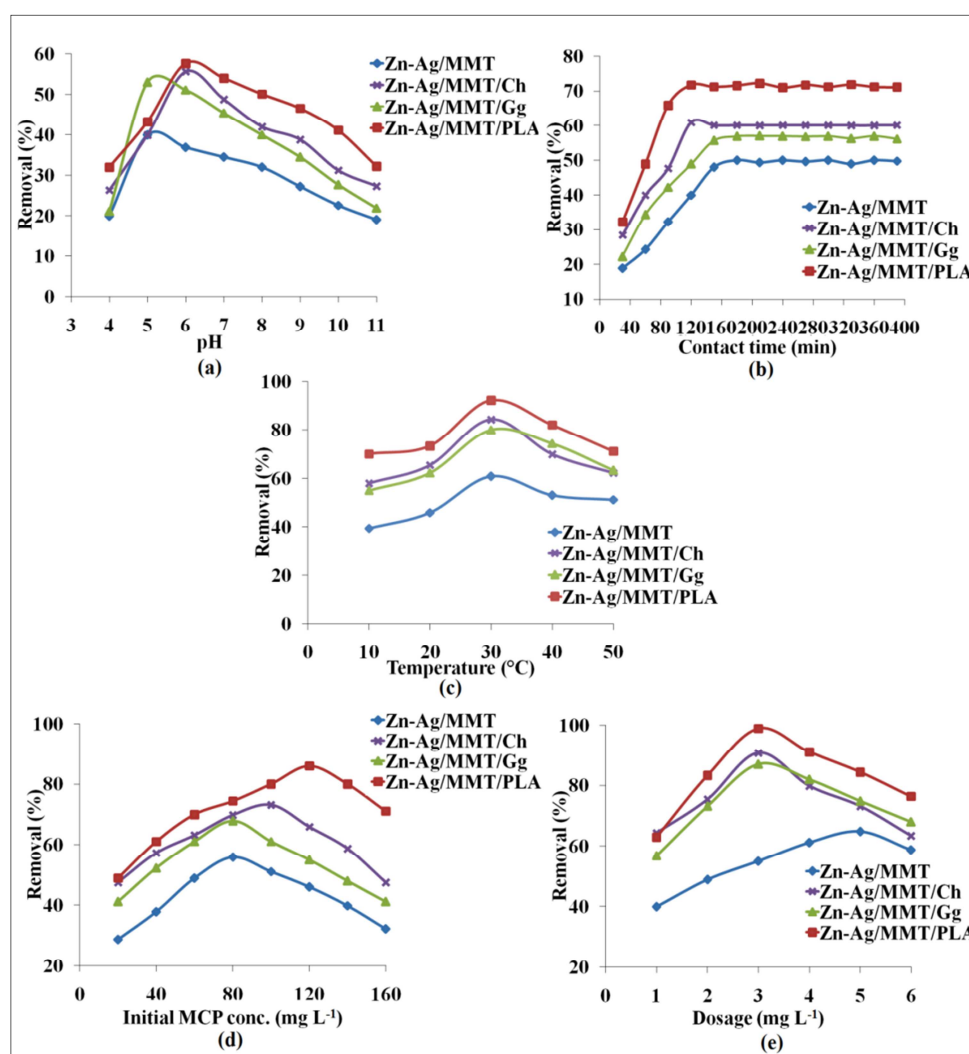


Figure 2: Effect of (a) pH, (b) contact time, (c) temperature, (d) initial MCP concentration and (e) dosage on removal of MCP

Equilibrium, kinetic and thermodynamic studies

The adsorption isotherm is an equilibrium relationship that correlates the amount of adsorbate on the adsorbent as a function of its concentration at constant temperature. Among the two parameter isotherms tested, Freundlich

isotherm model was found to exhibit the best fit with high correlation coefficient (R^2) and low error (APE) values thereby suggesting a heterogenous mode of MCP adsorption on all the composites (Fig. 3a). The results showed that the adsorption capacity was higher in case of Zn-Ag/MMT/PLA nanobiocomposite (high K_F value, 8.63) compared to other composites (Table 1). Langmuir isotherm model exhibited a poor fit with the experimental data due to low R^2 values and high error values. D-R isotherm model though having low error values exhibited a poor fit due to low R^2 values for all the composites.

In order to examine the diffusion mechanism involved during the adsorption process, various kinetic models were tested. The kinetic parameters including correlation coefficients (R^2), k_1 , k_2 and calculated $q_{e,cal}$ values of pseudo-first order, pseudo-second order and intraparticle diffusion are determined by linear regression as shown in Table 1. It can be observed that the $q_{e,cal}$ values of two kinetic models *viz.*, pseudo-first order and pseudo second order are very close to the experimental q_e values. Pseudo-first order exhibited best fit than pseudo second order with high R^2 and low error values suggesting the involvement of physical forces in the adsorption of MCP by all the composites (Fig. 3b). The nature of diffusion was evaluated by using intra-particle diffusion model and Boyd plot. Both the models exhibited a good linearity indicating their significant role and Boyd curves did not pass the through the origin, which suggested the involvement of both the diffusion mechanisms in adsorption of MCP by Zn-Ag/MMT composites (Fig. 3c-d).

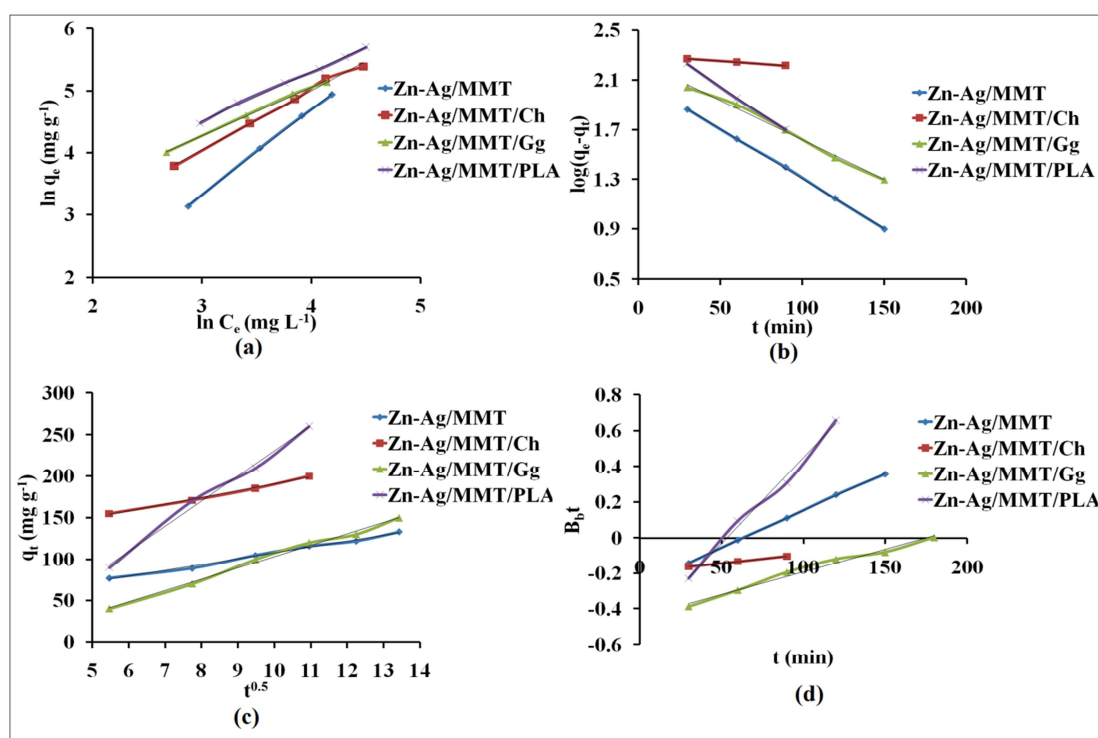


Figure 3: (a) Freundlich isotherm model, (b) Pseudo-first order, (c) intraparticle diffusion, (d) Boyd plot of MCP adsorption onto composites

The experimental data obtained at different temperature (10 to 50 °C) were used to estimate the thermodynamic parameters of adsorption and are presented in Table 2. The values of enthalpy entropy were calculated from the slope and intercept of the plot of $\log(q_e/C_e)$ vs $1/T$ (Fig. 4). The negative ΔG values of all the studied temperatures suggested that the adsorption of MCP onto composites were thermodynamically feasible and spontaneous. The positive values of ΔH indicated the adsorption of MCP was endothermic in nature and the adsorption capacity increased with increase in temperature. The positive values of ΔS , further suggested that the increased randomness at the solid and liquid interface during the adsorption of MCP by all the composites at 30 °C. Similar trend was observed for pesticide adsorption on artificially prepared resin [37].

Table 1 Equilibrium isotherm and kinetic model parameters for MCP adsorption on nanocomposite and nanobiocomposites

	Parameters	Zn-Ag /MMT	Zn-Ag /MMT/Ch	Zn-Ag/ MMT /Gg	Zn-Ag /MMT/PLA	
Isotherm Models	q_m (mg g ⁻¹)	142.8	200.0	166.6	333.3	
	Langmuir	K_L (L mg ⁻¹)	0.007	0.007	0.037	0.005
	R^2	0.97	0.98	0.99	0.99	
	APE (%)	32.8	29.0	6.64	3.85	
Freundlich	n	1.0	1.04	1.27	1.27	
	K_F (mg g ⁻¹)	2.25	3.26	6.86	8.63	
	R^2	0.99	0.99	0.99	0.99	
	APE (%)	19.3	3.53	2.04	1.64	
D-R	q_m (mg g ⁻¹)	126.5	177.6	156.9	258.7	
	E (KJ mol ⁻¹)	0.07	0.09	0.002	0.07	
	β (mol ² J ⁻²)	1*10 ⁻⁴	6*10 ⁻⁵	4*10 ⁻⁵	8*10 ⁻⁵	
	R^2	0.96	0.97	0.96	0.98	
	APE (%)	3.61	3.70	1.89	2.40	
Kinetic models						
Pseudo first order	q_e	128.5	197.6	180	251.1	
	K_1 (min ⁻¹)	0.01	0.01	0.013	0.018	
	R^2	0.99	0.99	0.99	0.99	
	APE (%)	1.52	14.3	3.66	1.06	
Pseudo second order	q_e	142.8	250	166.6	250	
	K_2 (g mg ⁻¹ min ⁻¹)	1*10 ⁻⁴	2*10 ⁻⁴	5*10 ⁻⁵	5*10 ⁻⁴	
	R^2	0.99	0.99	0.99	0.99	
	APE (%)	30.5	16.6	35.9	2.31	
Intra-particle diffusion	V	7.11	33.6	13.7	30.3	
	C	36.6	31.3	34.4	73.0	
	R^2	0.99	0.99	0.99	0.99	
	APE (%)	34.7	39.7	2.65	2.66	

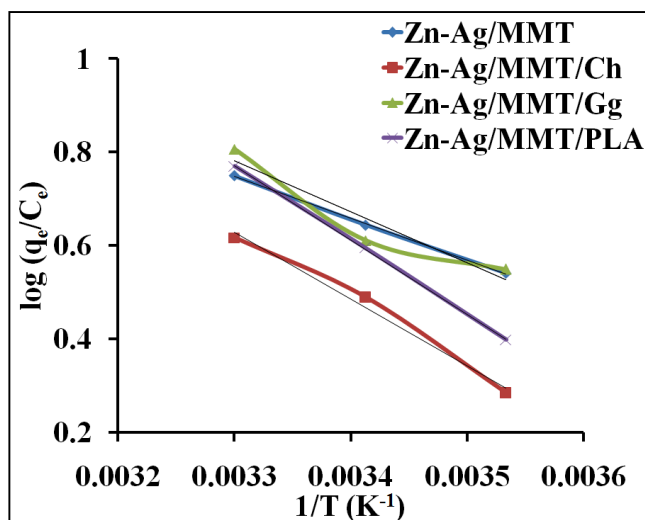


Figure 4: Thermodynamic studies of adsorption of MCP onto Zn-Ag/MMT composites

Table 2 Thermodynamic parameters of MCP adsorption onto Zn-Ag/MMT nanocomposite and nanobiocomposites

Composites	Temperature (K)	ΔH° (KJ mol ⁻¹)	ΔS° (KJ mol ⁻¹ K ⁻¹)	ΔG° (KJ mol ⁻¹)
Zn-Ag/MMT	283	+17.0	+0.07	-2.8
	293			-3.5
	303			-4.2
Zn-Ag/MMT/Ch	283	+27.3	+0.10	-1.0
	293			-2.0
	303			-3.0
Zn-Ag/MMT/Gg	283	+20.9	+0.08	-1.7
	293			-2.5
	303			-3.3
Zn-Ag/MMT/PLA	283	+30.4	+0.11	-0.7
	293			-1.8
	303			-2.9

Spectroscopic studies

FT-IR spectra representing various functional groups of Zn-Ag/MMT composites before and after MCP adsorption are shown in Fig. 5a-h. Major involvement of primary alcohols (O-H stretch) was observed in case of Zn-Ag/MMT and Zn-Ag/MMT/PLA (Fig. 5e and 5h). In case of Zn-Ag/MMT/Ch and Zn-Ag/MMT/Gg, amines (N-H stretch) were found to play a vital role in the MCP adsorption (Fig. 5f and 5g). Considerable stretches at 919.78, 912.23 837.77 and 832.46 cm^{-1} suggested the presence of alkenes on all composites thereby indicating the adsorption of MCP (Fig. 5e-h). A noticeable change in transmittance was found to be higher in case of Zn-Ag/MMT/PLA as compared to the other composites indicating the major participation of their functional groups in adsorption process.

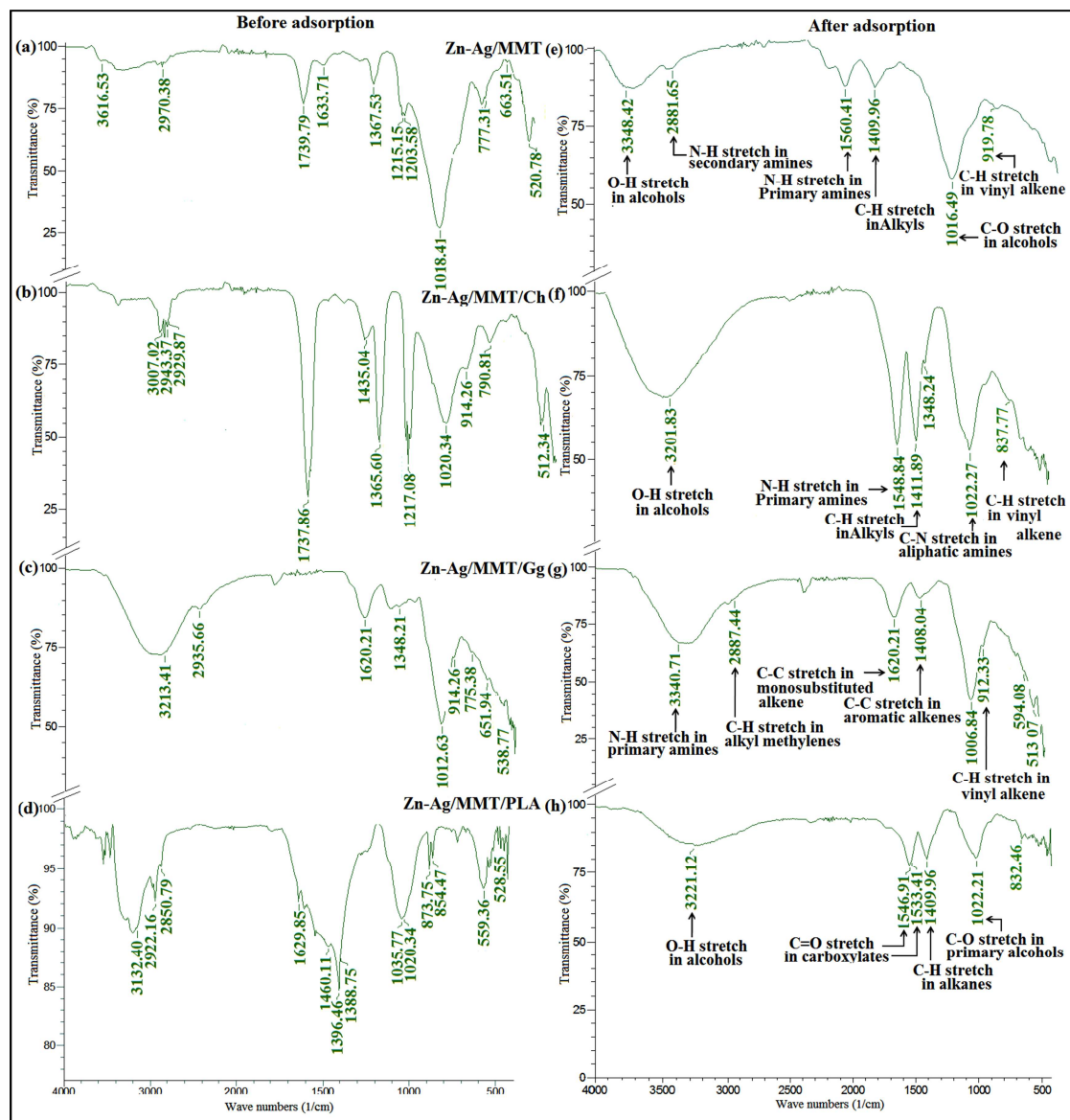


Figure 5: FT-IR analysis

AFM analysis was done to gain a deeper insight with respect to the surface properties in case of Zn-Ag/MMT/PLA nanobiocomposite before (Fig. 6a-b) and after (Fig. 6c-d) MCP adsorption. Homogenous distribution of Zn-Ag nanoparticles on the MMT/PLA surface was noted suggesting the homogenous surface roughness. The loss of surface roughness was noted which was due to the patchy and high surface coverage of adsorbed MCP.

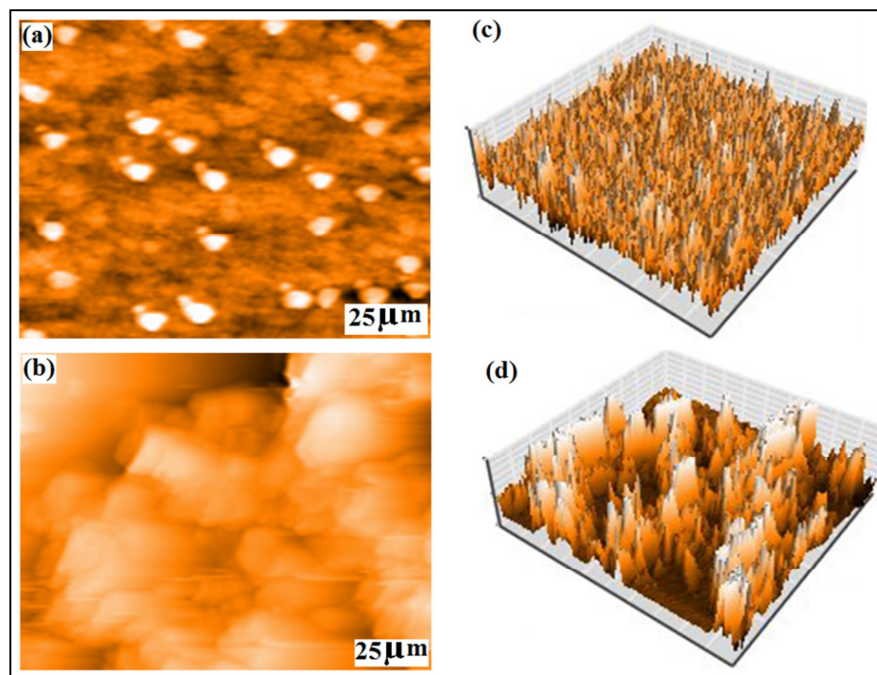


Figure 6: Surface topology of Zn-Ag/MMT/PLA (a) before and (b) after MCP adsorption. AFM images of 3d layer Zn-Ag/MMT/PLA (c) before and (d) after MCP adsorption

The changes in elemental composition of Zn-Ag/MMT/PLA nanobiocomposite surface before and after MCP adsorption were analysed using EDX (Fig. 7). The spectrum of Zn-Ag/MMT/PLA nanobiocomposite before adsorption showed the presence of C, O, Zn, Mg and Al elements on the surface (Fig. 7a). The adsorption of MCP was confirmed by the presence of P peak as shown in Fig. 7b. A significant decrease in C, Zn and Mg peak intensity was noted which confirmed their involvement in the MCP adsorption process. From EDX spectrum, it was clear that all the components in the nanobiocomposite played a significant role in the adsorption of MCP.

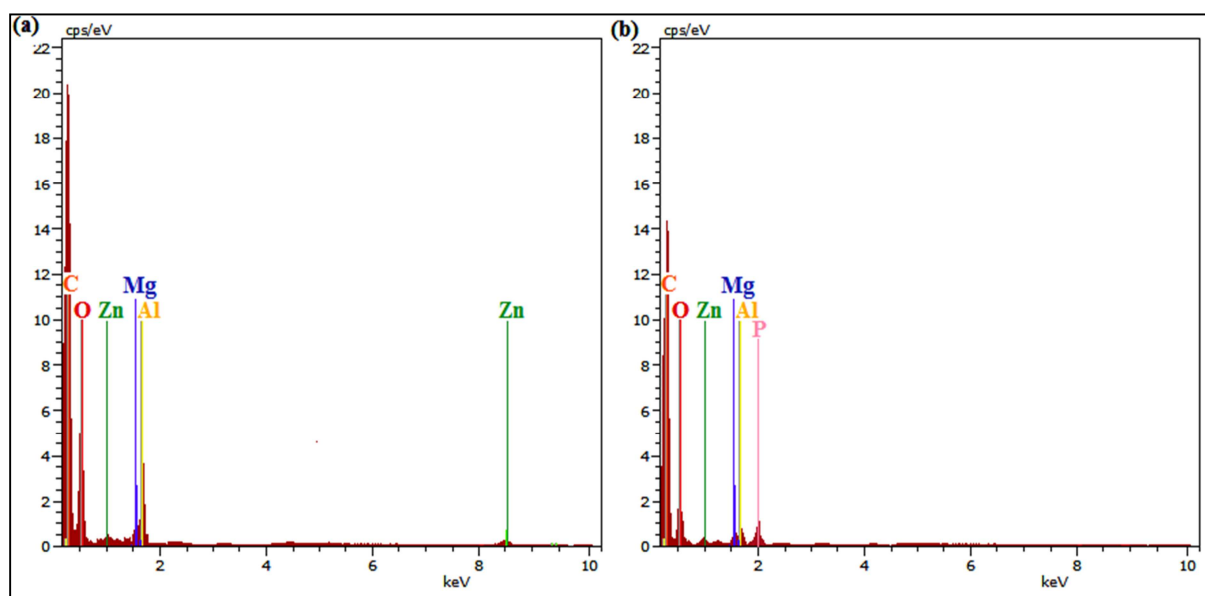


Figure 7: EDS spectra of Zn-Ag/MMT/PLA (a) before and (b) after MCP adsorption

Desorption and regeneration experiments

Desorption and regeneration experiments were conducted using deionised water as a desorbing agent. Eight cycles of adsorption and desorption were performed in a batch mode using a same composite and desorption reached within 60 min. From the Fig. 8, it was observed that the removal efficiency of Zn-Ag/MMT/PLA nanobiocomposite remains almost constant for first five cycles whereas, a gradual decrease was noted for successive cycles.

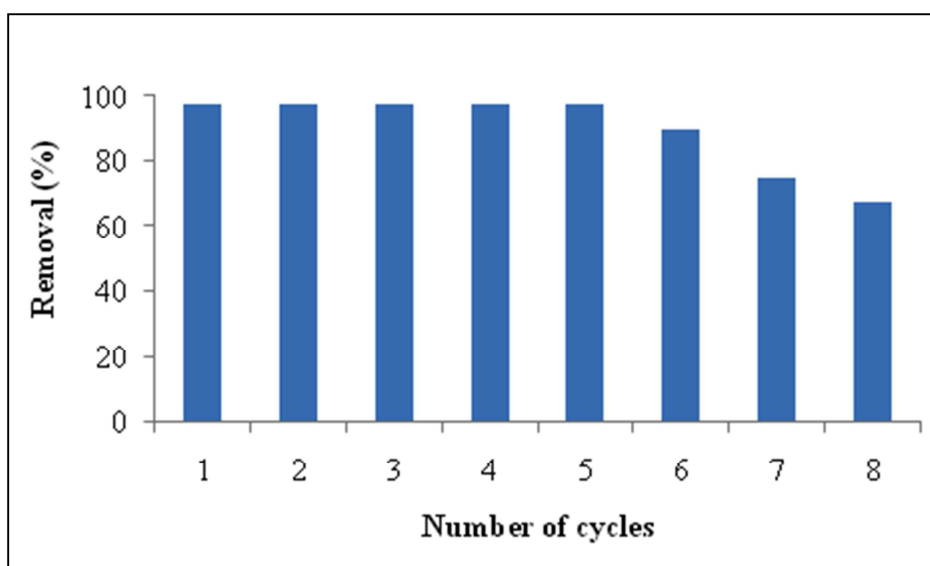


Figure 8: Regeneration studies

CONCLUSION

The results of the present study showed the application of bimetallic Zn-Ag nanoparticles embedded in MMT-biopolymer nanobiocomposites for the removal of MCP from aqueous environment. Maximum MCP removal was noted in case of Zn-Ag/MMT/PLA under optimized conditions. Equilibrium sorption data exhibited a best fit to the Freundlich isotherm model, indicating a heterogenous mode of adsorption of MCP onto the composites surface. The kinetic data indicated the involvement of physical forces by intra-particle and film diffusion modes during adsorption. Endothermic nature of the MCP adsorption was well defined by thermodynamic studies. Regeneration studies suggested that the Zn-Ag/MMT/PLA could be reused up to five cycles and could serve as potential remediation agent for the efficient removal of MCP from aqueous environment.

Acknowledgement

The authors gratefully acknowledge VIT University for providing necessary laboratory facilities for smooth conduct of work.

REFERENCES

- [1] J. Rachna, G. Veena, S.K. Pratap, G. Sheetal, *Int J Environ Sci.*, **2012**, 3, 841.
- [2] G. Velmurugan, D.D. Venkatesh Babu, S. Ramasamy, *Toxicology.*, **2012**, 307, 103.
- [3] X. Zhang, H. Tian, W. Wang, S. Ru, *Gen Comp Endocrinol.*, **2013**, 193, 158.
- [4] T.S. Bhalero, P.R. Puranik, *Int Biodeter Biodegradation.*, **2009**, 63, 503.
- [5] World Health Organization, **2011**, Non communicable diseases country profiles. WHO Global report, Geneva, Switzerland.
- [6] A.I. Kazi, A. Oommen, *Neurotoxicology.*, **2012**, 33, 156.
- [7] X. Zhang, L. Gao, K. Yang, H. Tian, W. Wang, S. Ru, *Comp Biochem Physiol C: Pharmacol Toxicol.*, **2013**, 157, 33.
- [8] Vismaya, P.S. Rajini, *Food Chem Toxicol.*, **2014**, 71, 236.
- [9] B.K. Avasarala, S.R. Tirukkavalluri, S. Bojja, *J Hazard Mater.*, **2011**, 186, 1234.
- [10] A. Amalraj, A. Pius, *J Water Process Eng.*, **2015**, 7, 94
- [11] X.H. Zhao, J. Wang, *Food Chem.*, **2012**, 131, 300.
- [12] G.E. Ustun, S.K.A. Solmaz, H.S. Azak, *Clean- Soil, Air, Water.*, 43, DOI: 10.1002/clen.201400139.
- [13] K. Sivagami, R.R. Krishna, T. Swaminathan, *J Water Sustainability.*, **2011**, 1, 75.
- [14] B.K. Singh, A. Walker, *FEMS Microbiol Rev.*, **2006**, 30, 428.
- [15] N. Badr, K.M. Al-Qahtani, *Environ Monit Assess.*, **2013**, 185, 9669.
- [16] C. Fuar, H.M. Pignon, P.L. Cloirec, *Adsorption.*, **2005**, 11, 479.
- [17] S. Polati, S. Anqioi, V. Gianotti, F. Gosetti, M.C. Gennaro, *J Environ Sci Health B.*, **2006**, 41, 333.
- [18] S. Senthilkumar, *Modern Appl Sci*, **2010**, 4, 67.
- [19] J. Pal, M.K. Deb, J.K. Sircar, P.K. Agnihotri, *Appl Water Sci*, **2015**, 5, 181.
- [20] R. Srinivasan, *Adv Mater Sci Eng*, **2011**, Article ID: 872531.
- [21] G. Crini, *Prog Polym Sci*, **2005**, 30, 38.

- [22] N. Bleiman, Y.G. Mishael, *J Hazard Mater.*, **2010**, 183, 590.
- [23] F.A.R. Pereira, K.S. Sousa, G.R.S. Cavalcanti, M.G. Fonseca, A.G. de Souza, A.P.M. Alves, *Int J Biol Macromol.*, **2013**, 61, 471.
- [24] R. Celis, M.A. Adelino, M.C. Hermosin, J. Cornejo, *J Hazard Mater*, **2012**, 209-210, 67.
- [25] S. M. Dehaghi, B. Rahmanifar, A.M. Moradi, P.A. Azar, *J Soudi Chem Soc.*, **2014**, 18, 348.
- [26] G.Z. Kyzas, D.N. Bikiaris, *Mar Drugs*, **2015**, 13, 312.
- [27] K.V. Srivatsan, R. Lakra, K.P. Sai, M.S. Kiran, *J Mater Chem: B.*, **2016**, 4, 1437.
- [28] J.E. Khalid, O.E. Gamal, S.D. Ramy, *Int J Miner Process.*, **2013**, 120, 26.
- [29] D. Charumathi, N. Das, *Desalination.*, **2012**, 285, 22.
- [30] M.V. Shankar, K.K. Cheralathan, B. Arabindoo, M. Palanichamy, V. Murugesan, *J Mol Catal A.*, **2004**, 223, 195.
- [31] J. Pal, M.K. Deb, J.K. Sirear, P.K. Agnihotri, *Appl Water Sci.*, **2015**, 5, 181.
- [32] V.K. Gupta, I. Ali, Suhas, V.K. Saini, *J Colloid Interface sci.*, **2006**, 299, 556.
- [33] M.E. Ouardi, S. Alahiane, S. Qourzal, A. Abamrane, A. Assabbane, J. Douch, *Am J Anal Chem.*, **2013**, 4, 72.
- [34] V.K. Singh, R.S. Singh, P.N. Tiwari, J.K. Singh, F. Gode, Y.C. Sharma, *J Water Resource Prot.*, **2010**, 2, 322.
- [35] D.J. Mall, V.C. Srivastava, N.K. Agarwal, *Dye Pigment.*, **2005**, 25, 210.
- [36] D. Das, G. Basak, V. Lakshmi, N. Das, *Biochem Eng J.*, **2012**, 64, 30.
- [37] M. Naushad, Z.A. AlOthman, M.R. Khan, *Talanta.*, **2013**, 115, 15.